

Discovery of the Longriba Fault Zone in Eastern Bayan Har Block, China and its tectonic implication

XU XiWei^{1†}, WEN XueZe², CHEN GuiHua¹ & YU GuiHua¹

¹ Institute of Geology, China Earthquake Administration, Beijing 100029, China

² Earthquake Administration of Sichuan Province, Chengdu 610041, China

Re-measured GPS data have recently revealed that a broad NE trending dextral shear zone exists in the eastern Bayan Har block about 200 km northwest of the Longmenshan thrust on the eastern margin of the Qinghai-Tibet Plateau. The strain rate along this shear zone may reach up to 4–6 mm/a. Our interpretation of satellite images and field observations indicate that this dextral shear zone corresponds to a newly generated NE trending Longriba fault zone that has been ignored before. The northeast segment of the Longriba fault zone consists of two subparallel N54°±5°E trending branch faults about 30 km apart, and late Quaternary offset landforms are well developed along the strands of these two branch faults. The northern branch fault, the Longriqu fault, has relatively large reverse component, while the southern branch fault, the Maoergai fault, is a pure right-lateral strike slip fault. According to vector synthesizing principle, the average right-lateral strike slip rate along the Longriba fault zone in the late Quaternary is calculated to be 5.4±2.0 mm/a, the vertical slip rate to be 0.7 mm/a, and the rate of crustal shortening to be 0.55 mm/a. The discovery of the Longriba fault zone may provide a new insight into the tectonics and dynamics of the eastern margin of the Qinghai-Tibet Plateau. Taken the Longriba fault zone as a boundary, the Bayan Har block is divided into two sub-blocks: the Ahba sub-block in the west and the Longmenshan sub-block in the east. The shortening and uplifting of the Longmenshan sub-block as a whole reflects that both the Longmenshan thrust and Longriba fault zone are subordinated to a back propagated nappe tectonic system that was formed during the southeastward motion of the Bayan Har block owing to intense resistance of the South China block. This nappe tectonic system has become a boundary tectonic type of an active block supporting crustal deformation along the eastern margin of the Qinghai-Tibet Plateau from late Cenozoic till now. The Longriba fault zone is just an active fault zone newly-generated in late Quaternary along this tectonic system.

Qinghai-Tibet Plateau, active block, newly-generated fault zone, slip rate, nappe tectonics

The Cenozoic tectonic deformation pattern of the eastern Qinghai-Tibet Plateau has attracted great attention of geologists from all over the world. This aspect has a direct influence on the discussion about the dynamic model of the Qinghai-Tibet Plateau, including both the current theories of lateral escape tectonics and crustal thickening. Among them, the theory of lateral escape tectonics lays emphasis on the eastward extrusion of the blocks of various orders in the Qinghai-Tibet Plateau through rapid slip along large-scale strike slip faults, which accommodate the south-north crustal shortening

of the plateau^[1–5]. In contrast, the theory of the crustal thickening emphasized that the northward movement of the Indian plate has caused the thickening of the ductile lower crust and the development of numerous faults, along which the slow motion has resulted in distributed continuous deformation^[6–10]. However, it is difficult at

Received August 30, 2007; accepted January 18, 2008

doi: 10.1007/s11430-008-0097-1

†Corresponding author (email: xiweixu@vip.sina.com)

Supported by the National Basic Research Program of China (Grant No. 2004CB418401) and the National Natural Science Foundation of China (Grant No. 40474037)

present to conclude which one of the above dynamic models conforms better with the actual situation, as neither model has discussed its effect on the tectonic deformation and kinematics along the eastern margin of the Qinghai-Tibet Plateau.

Many studies have been done on tectonic frameworks of the Qilianshan region on the northeastern edge of the Qinghai-Tibet Plateau, and on the tectonic framework of the Sichuan-Yunnan rhombic block on the southeastern edge of the plateau^[1-17]. Moreover, the segmented activity of the Longmenshan thrust at the easternmost end of the Bayan Har block and its relation to seismicity have also been discussed^[18-24], while the rapid uplift process of the Longmenshan sub-block, including the Longmenshan thrust and Minjiang fault, has been analyzed as well^[25,26]. However, little is known about distribution of active faults in the region to the west of Longmenshan. Recently, GPS re-measurements by China Crustal Movement Observation Network not only have provided information about the current motion of the blocks of various orders in Longmenshan and its adjacent areas as well as the present-day strain rate along the known active faults^[27-31], but also revealed existence of a NE-trending dextral shear zone subparallel to the Longmenshan thrust west of the Longmenshan thrust and Minjiang fault. The strain rate along this shear zone is estimated to be 4–6 mm/a^[29,31]. Interpretation of satellite images and field investigations show that the dextral shear zone revealed by the GPS re-measurements corresponds spatially to a NE-trending Longriba fault zone at the eastern end of the Bayan Har block. However, little is known about the Longriba fault zone so far, as the fault zone is located at a remote area of the Qinghai-Tibet Plateau. In light of the latest results of our investigations, here we will first demonstrate the geometric features and the average late Quaternary slip rate of the Longriba fault zone, and then, together with the regional tectonic setting, discuss the latest tectonic deformation pattern at the eastern end of the Bayan Har block, as well as the tectonic process and its implication along the Longriba fault zone. All these results may shed new light on the tectonic deformation pattern and dynamic model of the Qinghai-Tibet Plateau.

1 Tectonic setting

The Bayan Har block is an elongated tectonic domain that is bounded by the NWW-trending Kunlun,

Garzê-Yushu and Xianshuihe faults, the southwest segment of the NE-trending Longmenshan thrust, and nearly SN-trending Minjiang fault, located at the central easternmost Qinghai-Tibet Plateau (Figure 1). On the basis of the measurements of geomorphic offsets, the Holocene left-lateral slip rate along the Garzê-Yushu and Xianshuihe faults has been estimated to be 12 ± 2 mm/a^[15,32], to be 11.5 ± 2 mm/a along the main part of the Kunlun fault^[33], but its slip rate along the segment to the east of Maqen Town decreases significantly^[34]. The GPS left-lateral rate for these two NWW-trending strike slip faults is about 10 mm/a^[30,31], indicating that the long term geologic slip rate is basically consistent with the GPS rate. In addition, the Longmenshan thrust is characterized by faulting segmentation in Quaternary. The northeast segment of the Longmenshan thrust to the north of Anxian County is an inactive segment during late Quaternary, displaying relatively weak seismicity^[23,24]. In contrast, the southwest segment of the Longmenshan thrust to the south of Anxian County has been active since late Pleistocene^[35], which is demonstrated by cutting the upper Pleistocene, and has become the boundary between the Chengdu plain and the plateau in the northwest with great difference in height. It is also the active segment that historical and present-day earthquakes often strike^[24]. The nearly SN-trending Minjiang fault consists of the Minjiang and Huya secondary faults. The former is located to the north of Songpan Town, and is dominated by thrusting, with vertical slip rate of 0.4–0.5 mm/a. The latter is located to the southeast of Songpan Town, dominated by left-lateral strike slip, having a horizontal slip rate of about 1.4 mm/a^[36] (Figure 1).

The newly discovered Longriba fault zone on the western side of the Minjiang fault has cut the Bayan Har block into two sub-blocks: the Ahba sub-block in the west and the Longmenshan sub-block in the east. Of the two, the Ahba sub-block is the main body of the Bayan Har block, and the eastward present-day translation velocity of this sub-block is about 11.4 mm/a. In contrast, the translation direction of the Longmenshan sub-block is N116°E, and its velocity is about 8.5 mm/a^[29,31]. This may reflect that the southeastward translation velocity has decreased for about 4 mm/a within the range of 200 km-wide in the Longmenshan sub-block^[30,36]. Available data have shown that the decrease of the velocity in the two adjacent sub-blocks in east Bayan Har block has been transformed mostly into the right-lateral faulting and thrusting along the Longriba fault zone, and the re-

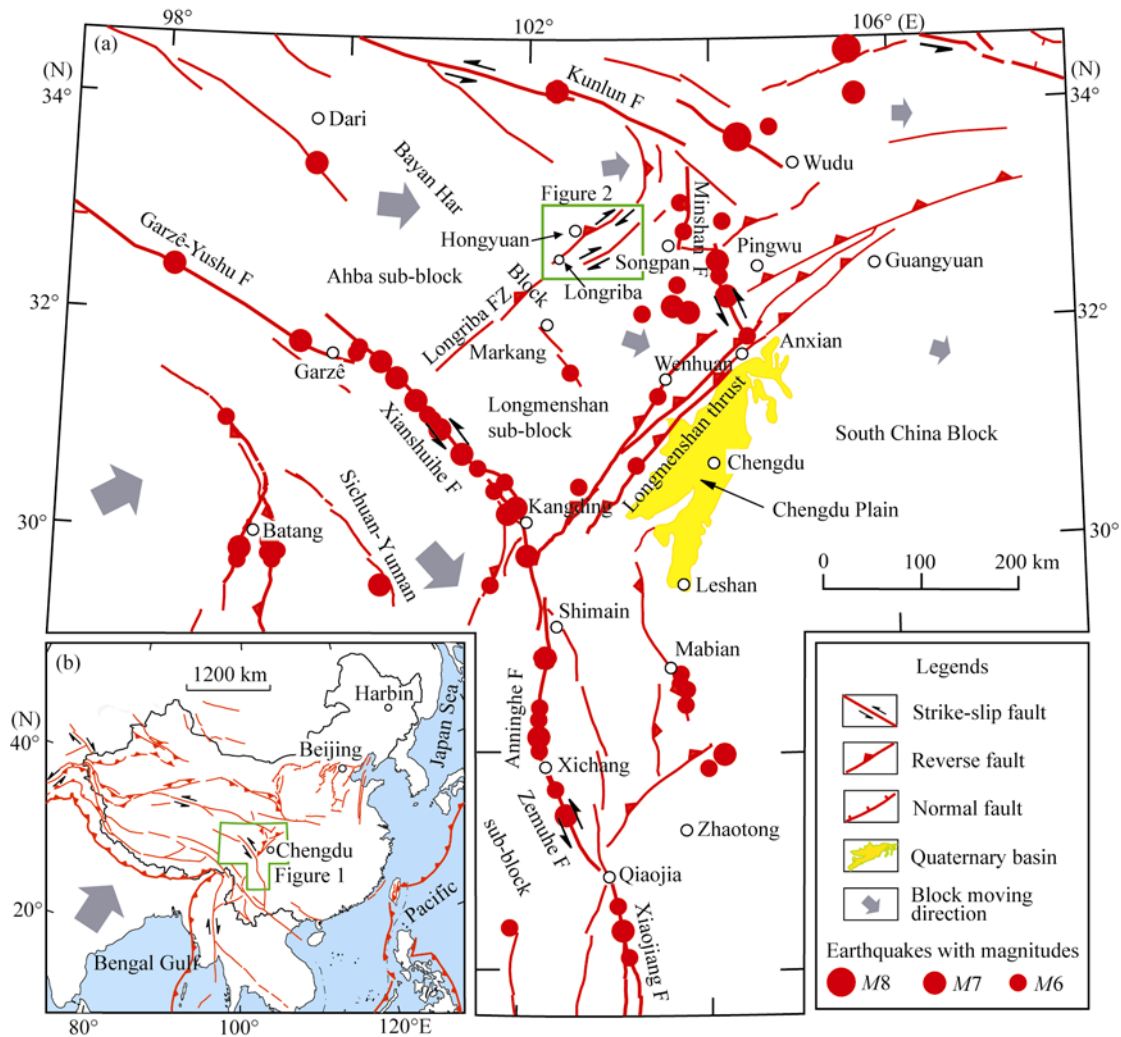


Figure 1 (a) Map showing distribution of active tectonics and earthquakes in the northwestern Sichuan Province and its adjacent areas; (b) index map of the studied area (Some seismic data are from ref. [37]). F, fault.

maining has been absorbed by the NE-trending Longmenshan thrust and other tectonic deformation in its adjacent areas.

2 Basic features of the Longriba fault zone

2.1 Geometric structure and kinetic property

The Longriba fault zone is an active fault zone that has been ignored before. Satellite images and field investigations have revealed that the Longriba fault zone is located about 200 km to the northwest of the Longmenshan thrust and to the west of Songpan and Markang Counties in the Plateau, and is called Longriba fault zone as it runs through the Longriba grasslands in Hongyuan County (Figure 1).

The northeast segment of the Longriba fault zone

extends in the Longriba grasslands and its northeastern adjacent areas, and consists of two $N54^{\circ}\pm 5^{\circ}E$ -trending sub-parallel branch faults about 30 km apart: the Longriqu fault (F1) in the north and the Maoergai fault (F2) in the south (Figure 2(a)), displaying southeastward thrusting and left-lateral strike-slip faulting, respectively. The Longriqu fault starts from the Longriba Town, and extends northeastward along the southeastern piedmont of the NE-trending Luolaoshan Range, having a total length of more than 100 km. Offset landforms show that this fault is a right-lateral strike slip fault with reverse component. At observation sites A ($102^{\circ}30'05.1''E$, $32^{\circ}32'21.6''N$) and B ($102^{\circ}28'25.1''E$, $32^{\circ}31'38.2''N$) to the east of Gema Village, the Longriqu fault dips toward the NW at an angle of $45^{\circ}-50^{\circ}$. At other sites to the west of the Gema Village, it is observed that the fault dissects the diluvium along the mountain piedmont,

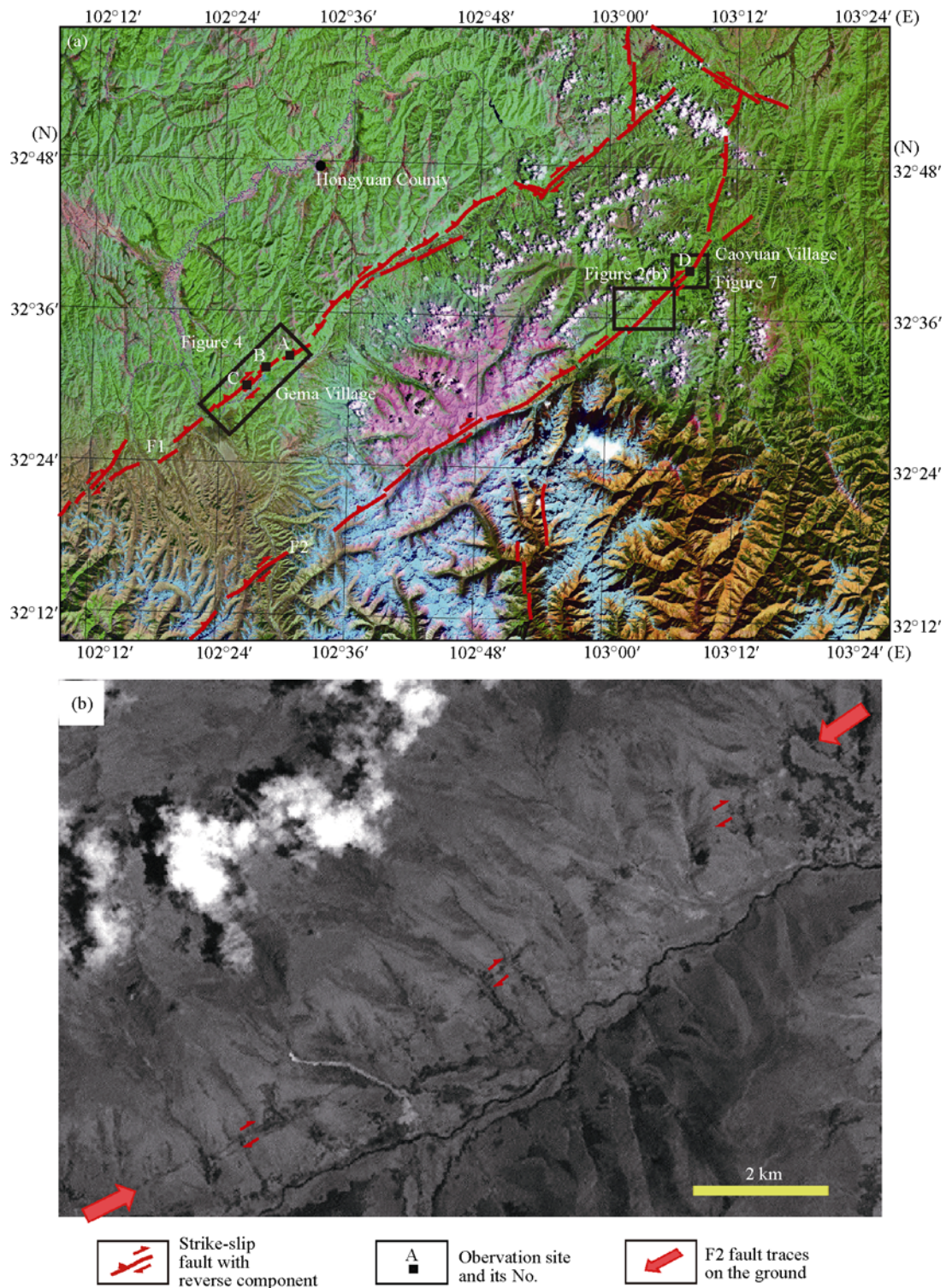


Figure 2 (a) Geometric structure of the northeast segment of the Longriba fault zone from interpretation of the ETM satellite images; (b) local satellite image showing linear offset landforms along the Maoergai fault. F1, Longriqu fault; F2, Maoergai fault.

having a maximum dip angle of about 60° (Figure 3). The Maoergai fault, the southern branch, extends also along a NE direction and cuts ridges and gullies to form a relatively straight linear feature (Figure 2(b)). Offset

landforms show that it is a pure right-lateral strike slip fault. Moreover, the strikes of both the Longriqu and Maoergai faults have turned to NNE or even to nearly SN at their northeast ends, and finally both faults are

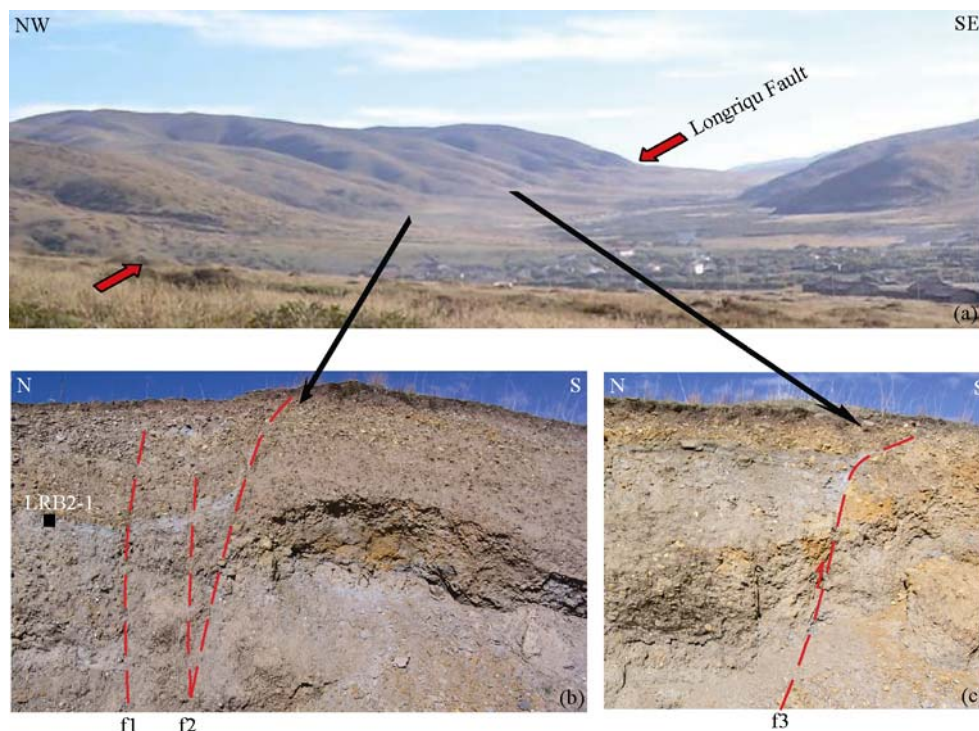


Figure 3 (a) Distant view of tectonic landforms along the Longriqu fault; (b) cross section of the site indicated by black arrow in (a), where several secondary faults cut diluvium; (c) cross section of a high dip-angle reverse fault indicated by black arrow in (a). Red arrow indicates the location of the Longriqu fault; red line with single arrow represents reverse fault and black square indicates the sampling site and number of the charcoal-bearing sample. f1, f2 and f3 are secondary faults of the Longriqu fault.

dissected by the southern branch faults of the NWW trending Kunlun fault.

The southwest segment of the Longriba fault zone extends in the area between the Longriba grasslands and the Xianshuihe fault to the northeast of the Luhuo County, where the two branch faults have disappeared, instead of a NE-trending newly generated strike slip fault, which is relatively simple and extends discontinuously. On the ETM satellite images this fault appears as distinct but discontinuous linear offset landforms, but has not yet been confirmed by field investigation (Figure 1).

2.2 Average late Quaternary slip rate

Field investigations indicate that along the strands of the Longriqu and Maoergai faults, offset landforms are well developed and distinct, which may provide reliable data for estimating average late Quaternary slip rate for the two branch faults and for analyzing tectonic deformation pattern along the boundary between the sub-blocks within the Bayan Har block.

2.2.1 Longriqu fault

Along the southeastern piedmont of Luolaoshan Range, north of Longriqu River, three levels of alluvial fans are

pervasively developed, while three levels of fill-cut terraces (T1, T2 and T3) are developed along large gullies and streams. The Longriqu fault systematically dissects various geologic bodies or morphologic units, such as pre-Quaternary bedrocks, Quaternary diluvial fans and terraces etc, resulting in various offset landforms such as cliff and fault scarps.

At observation site A (32°32'21.6"N, 102°30'05.1"E) to the east of the Gema Village, the Longriqu fault consists of two sub-parallel secondary faults (f1 and f2) (Figure 4). Of them, the northwestern one (f1) cuts the gully and T1 and T2 terraces on both its sides (Figure 5(a)), and a water fall scarp of 1 m high is formed at the site where the fault runs through the current gully. The T2/T1 riser on the western side is left-laterally offset by 11.5 ± 1.5 m (Figure 5(a)), and an older terrace T3 is offset vertically about 2.7 m. In addition, the other one (f2) on the southeastern side cuts an older alluvial fan, which corresponds to T3 terrace deposits. The right-lateral displacement of its eastern edge of the fan is about 28 m, while the vertical offset of the fan surface is about 6.3 m. At this site, a charcoal sample (LRB2-4) collected from an eroded, and then redeposited, gravel bed at the top of T2 terrace deposits yields a ^{14}C age of

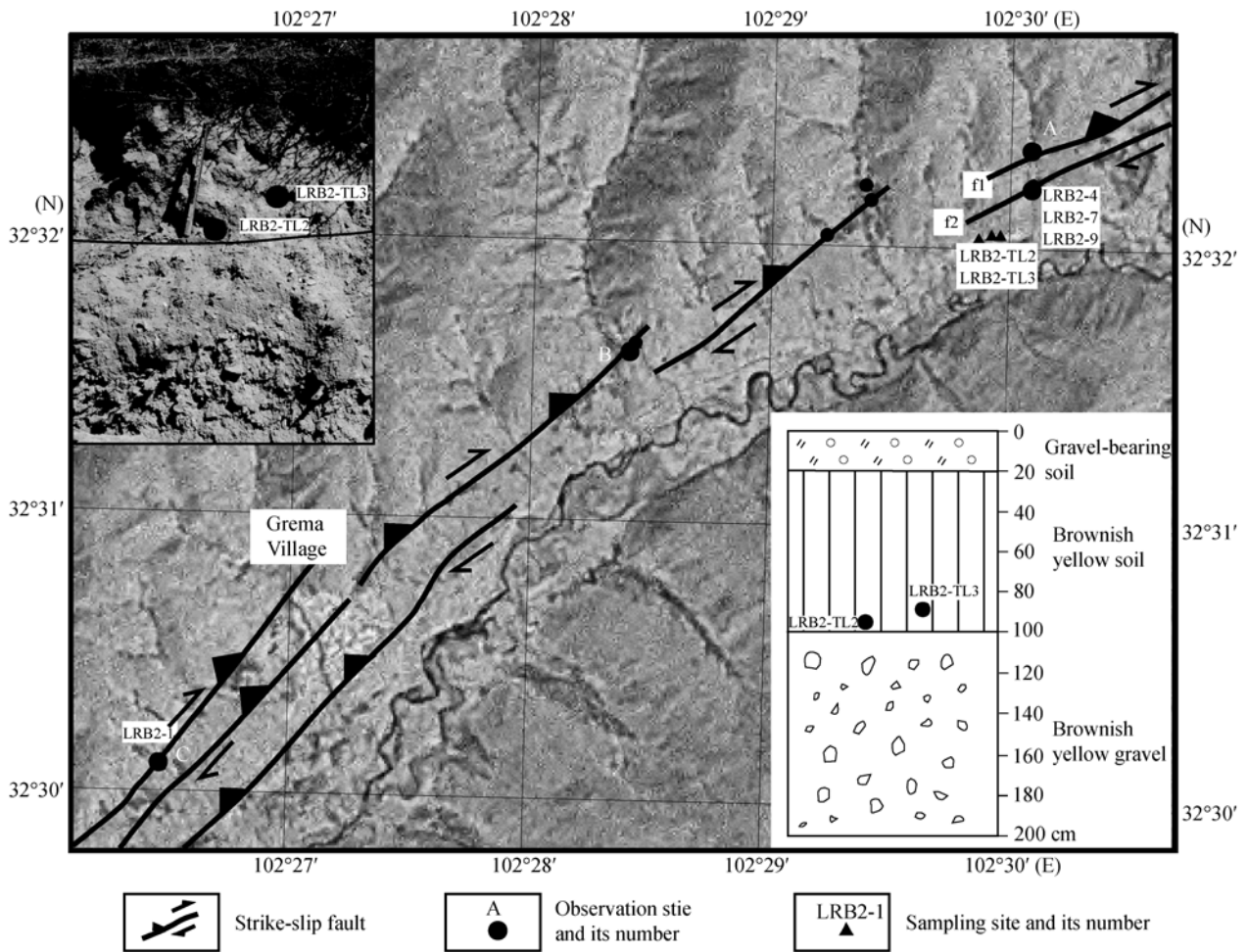


Figure 4 ETM satellite image of the the Longriqu fault traces in the vicinity of the Gema Village (location is shown in Figure 2). At the upper left corner is the photo of the sampling sites on T3 pluvial fan, and at the lower right corner is the stratigraphic cross section of sampling sites on T3 pluvial fan.

6660±40 a BP or a calibrated age of 5660—5510 cal a BP (Figure 5(b), Table 1), indicating that the terrace was formed earlier than this time. On the cross section of the western bank of the gully about 200 m to the south of the observation site A (Figure 5(c)), it is observed that the branch fault f2 dips toward NW at an angle of about 50° and cuts a dark grey sandy clay bed at the top of the T2 terrace. The ¹⁴C age of a charcoal sample (LRB2-9) collected from the upper part of the dark grey clay layer is 8985±50 a BP, whose calibrated age is 8300—8160 cal a BP (Table 1). However, the fault f2 is covered with grayish brown gravel-bearing soil layer, and a charcoal sample (LRB2-7) collected from the upper part of this layer yields the ¹⁴C age of 3935±35 a BP or calibrated age of 2580—2340 BC (Table 1). It is postulated, therefore, that the older age might represent the formation time of the T2 terrace, while the younger age represent the T1 terrace. Moreover, at the road side to the south of

the observation site A, the ages of two loess-like samples (LRB-TL2 and LRB-TL3) taken from the top of an old pluvial fan that corresponds to T3 terrace, whose sampling locations are shown on the inset of Figure 4 and Table 2, are dated by using optical stimulated luminescence (OSL) technique to be 15.5±1.7 ka and 11.1±1.2 ka, respectively. In the vicinity of observation site C (32°32'13.0"N, 102°29'23.7"E) along the piedmont to the west of the Gema Village, a gray charcoal-bearing mud bed of several centimeters in thickness exists at about 50—60 cm deep in gravel layer on the top of an old pluvial fan corresponding to T3 terrace (Figure 3(b)). A charcoal sample (LRB2-1) here yields a ¹⁴C age of 10670±100 a BP, whose calibrated age is 12633—12830 cal a BP (Figure 3 and Table 1). Based on the calibrated age of the charcoal samples and the OSL ages of the overlying loess-like samples, it is postulated that the old pluvial fan (T3) was formed in

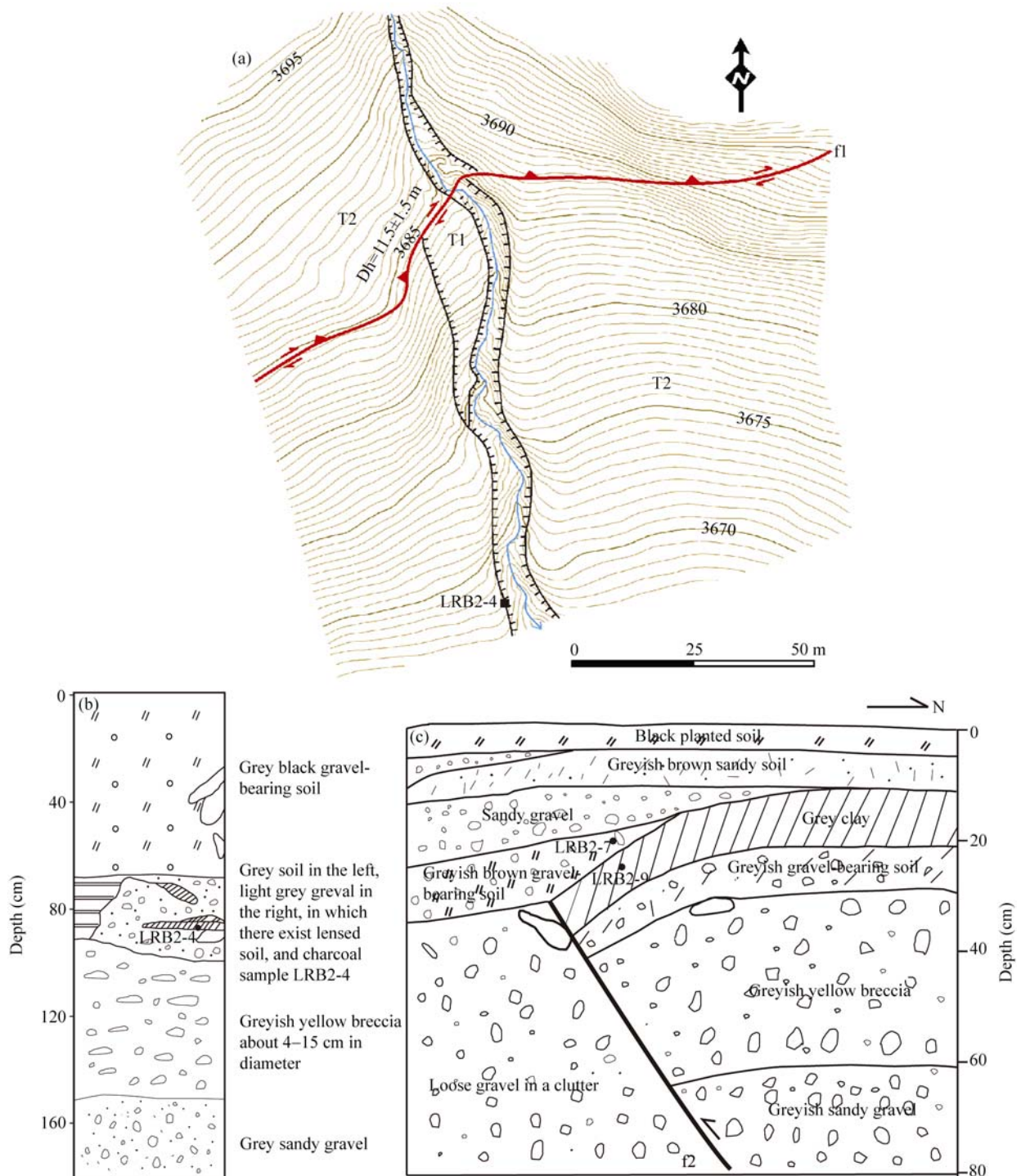


Figure 5 (a) Measured offset landforms along the branch fault f1 at observation site A by using Total Station; (b) cross section of the sampling locations for LRB2-4 sample on T2 terrace; (c) cross section of the sampling locations for samples LRB2-7 and LRB2-9. Red line represents the fault f1; T1 and T2 represent the terraces from young to old, respectively; Dh indicates cumulative right-lateral displacement in meter. The location of Figure 5(a) is at site (102°30'05.1"E, 32°32'21.6"N), and Figure 5(b) and 5(c) is at (102°30'05.9"E, 32°32'13.5"N).

post-glacial period, i.e. about 13.1 ± 1.7 ka BP.

In the vicinity of the observation site A, there are mainly fluvial geomorphic units. Therefore, the average late Quaternary slip rate for the active faults here should

be the ratio of the cumulative displacement of the alluvial-pluvial fan to its initial offset age. The initial offset age for the T_n/T_{n+1} terrace riser is equivalent to the aggradation phase of the younger terrace (T_n), while that

for a fluvial fan is close to the terminal aggradation phase of the fan itself^[16]. Based on the dating results of the samples from various morphologic surfaces at the observation site A, the incision and formation time of the T2 terrace is close to the age of the LRB2-9 sample (8230±70 cal a BP) (Table 1). Since the T2 terrace corresponds to the contemporaneous pluvial fan and T1 is a fill-cut terrace, the cumulative right-lateral offset of the T2/T1 riser, in fact, is equal to the cumulative offset of the eastern edge of the T2 contemporaneous pluvial fan (Figure 5(a)). From the horizontal cumulative displacement of 11.5±1.5 m for the T2 fan, therefore, the Holocene right-lateral slip rate for the fault f1 can be estimated to be 1.4±0.2 mm/a, and the vertical slip rate can be estimated to be 0.2 mm/a on the basis of 2.7 m vertical cumulative offset and 13.1±1.7 ka BP age of the T3 pluvial fan. Similarly, the average right-lateral slip rate for the branch fault f2 can be estimated to be 2.1±0.2 mm/a, and vertical slip rate to be 0.7±0.04 mm/a. At observation site A, therefore, the average right-lateral slip rate for the Longriqu fault since late Pleistocene should be 3.4±0.1 mm/a, and the vertical slip rate should be about 0.7 mm/a.

The observation site B (32°31'37.5"N, 102°28'25.7"E) is located at the outlet of a gully to the northeast of Gema Village, where the Longriqu fault has cut three phases of alluvial and pluvial fans, resulting in two sub-parallel fault scarps (Figure 6(a)), which offset right-laterally the T3/T2 riser for 33 m in total, and off-

set vertically the T2 for about 2.6 m and 2.8 m, respectively (Figure 6(b)), making a total vertical offset of 5.4 m. As mentioned earlier, the formation time of the T2 terrace at observation site A is 8230±70 cal a BP, and hence the Holocene right-lateral slip rate of the Longriqu fault at observation site B can be estimated to be about 4.0 mm/a, and the vertical slip rate to be about 0.66 mm/a. In addition, in the cross section of the gully on eastern side, it is observed that the southern fault scarp is controlled by a NW trending reverse fault with 48° dip angle. Providing that the Longriqu fault is NW dipping at an average angle of 50°, then the NW-SE crustal shortening rate caused by reverse faulting can be estimated to be about 0.55 mm/a.

2.2.2 Maoergai fault

The Maoergai fault extends along the bedrock canyon of the upper reach of the Maoergai River (Figure 2(b)), which is the tributary of the Heishui River, and its tributary, the Yanghonggou gully. Along the fault trace, right-lateral offset landforms are well developed, indicating that the Maoergai fault is a pure strike slip fault. Field observation has revealed that on the western bank of the main river at Caoyuan Village about 9 km to the northeast of the Maoergai Twon, five alluvial terraces have been developed (Figure 7). The Maoergai fault has cut systematically all these terraces, resulting in a low fault scarp with south-dipping free faces. For example, the south-dipping fault scarp on T3 terrace is about

Table 1 Radiocarbon samples and their ¹⁴C and calibrated ages^{a)}

Sample	Location		¹⁴ C age ±σ (a BP)	Calibrated age (cal a BP)	
	Latitude (N)	Longitude (E)		1σ(probability)	2σ(probability)
LRB2-01*	32°32'13.0"	102°29'23.7"	10670±100	12421–12435 BC (4.0%)	12633–12830 (96%)
LRB2-04	32°32'13.6"	102°30'05.9"	6660±40	5630–5555 BC (68.2%)	5660–5510 (95.4%)
LRB2-07	32°31'38.1"	102°28'26.2"	3955 ± 35	2500–2450 BC (32.6%)	2580–2340 (95.4%)
LRB2-09	32°31'38.1"	102°28'26.2"	8985 ± 50	8290–8200 BC (55.0%)	8300–8160 (62.7%)
MLG-1	32°39'55.1"	103°07'48.0"	4480 ± 40	3340–3210 BC (45.2%)	3350–3080 (87.1%)

a) The sample marked with * was dated by ¹⁴C Dating Laboratory of the Institute of Geology, China Earthquake Administration, and the other samples were dated by the AMS Laboratory of the Peking University. δ¹³C=−25‰. Calibration is carried out by using the OxCal v3.10 program (C. B. Ramsey, 2005, www.rlaha.ox.ac.uk/orau/oxcal.html).

Table 2 Ages of the samples by using optically stimulated luminescence (OSL) dating

Sample	Buried depth (m)	Measurement method	Equivalent dose (Gy)	α counting rate (cpks)	K (%)	Water content (%)	α coefficient	Dose rate (Gy/ka)	Age (ka)
LRB2-TL2	0.98	SMAR	63.2±2.3	9.3	2.2	4	0.04±0.02	4.1±0.4	15.5±1.7
LRB2-TL3	0.85	SMAR	43.6±1.3	10.3	2.0	14	0.04±0.02	3.9±0.4	11.1±1.2
MLG-TL1	1.80	SMAR	57.1±2.8	11	2.1	19	0.04±0.02	4.0±0.4	14.3±1.6
MLG-TL2	5.0	SMAR	294.2±15.9	10.9	2.0	17	0.04±0.02	4.1±0.4	74.5±8.5
MLG-TL3	1.6	SMAR	82.3±3.1	9.7	2.3	17	0.04±0.02	4.1±0.4	20.7±2.2

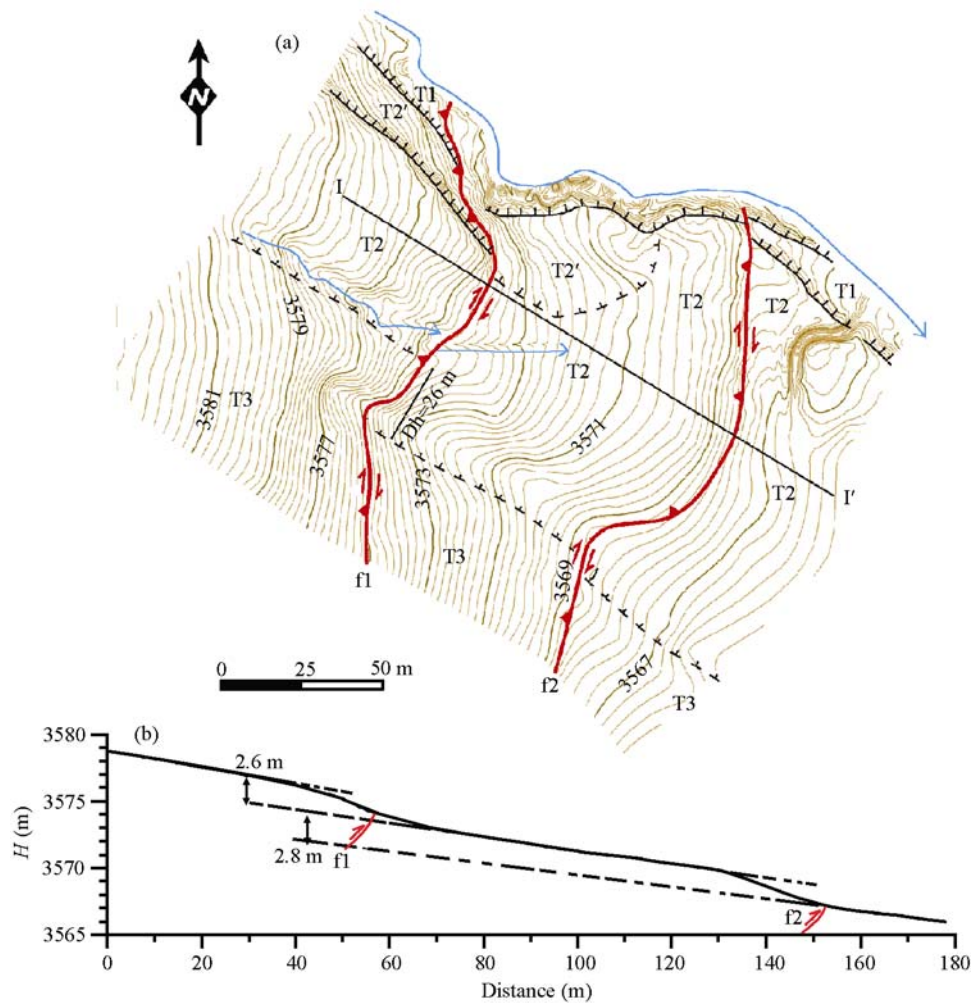


Figure 6 (a) Measured offset landforms along the Longriqu fault at observation site B by using Total Station; (b) I-I' topographic profile across the T2 terrace (legends are the same as in Figure 5).

20 cm high (Figure 8). Field measurement by interpretation of ETM satellite image obtains a cumulative right-lateral displacement of 225 ± 15 m for the T5/T4 riser (Figure 7). The cumulative right-lateral displacement for T3/T2 riser is measured by Total Station as 48 ± 5 m (Figure 8). At this site, the oldest terrace (T5) is overlain by brownish yellow loess layer of 4m thick. The age of a loess sample (MLG-TL1) collected at depth of about 2 m from the terrace surface at observation site ($32^{\circ}39'36.3''\text{N}$, $103^{\circ}07'42.4''\text{E}$) is dated by OSL method to be 14.3 ± 1.6 ka (Table 2). At observation site ($32^{\circ}39'37.9''\text{N}$, $103^{\circ}07'41.3''\text{E}$), the sample (MLG-TL2) collected at the contact between the brownish yellow loess and fluvial gravel layer at 4m deep below the terrace surface is dated to be 74.5 ± 8.5 ka, which represents the formation time of the T5 terrace. The T5/T4 terrace riser is about 30 m high. The observation site

($32^{\circ}39'52.1''\text{N}$, $103^{\circ}07'42.6''\text{E}$) is located on the T4 terrace. The age of the sample (MLG-TL3) collected from about 1.6m below the T4 terrace at the contact between the clay layer of flood plain facies and the underlying fluvial gravel layer is dated by OSL method to be 20.7 ± 2.2 ka, which might represent the terminal aggradation phase of the T4 terrace and its sampling cross section is shown on inset diagram in Figure 7). The ^{14}C age of a charcoal sample (MLG-1) collected from the clay layer at about 2 m depth below the T3 terrace is 4480 ± 40 a BP (Table 1). Because the sampling location has not reached the top part of the fluvial gravel layer of the T3 terrace, it is believed that the age of the sample is younger than its formation age. Both the T4 and T3 terraces are fill-cut terraces that were formed by eroding the T5 terrace. On the northern wall of the fault, the T4/T3 riser is about 3 m high (Figure 8), and on the

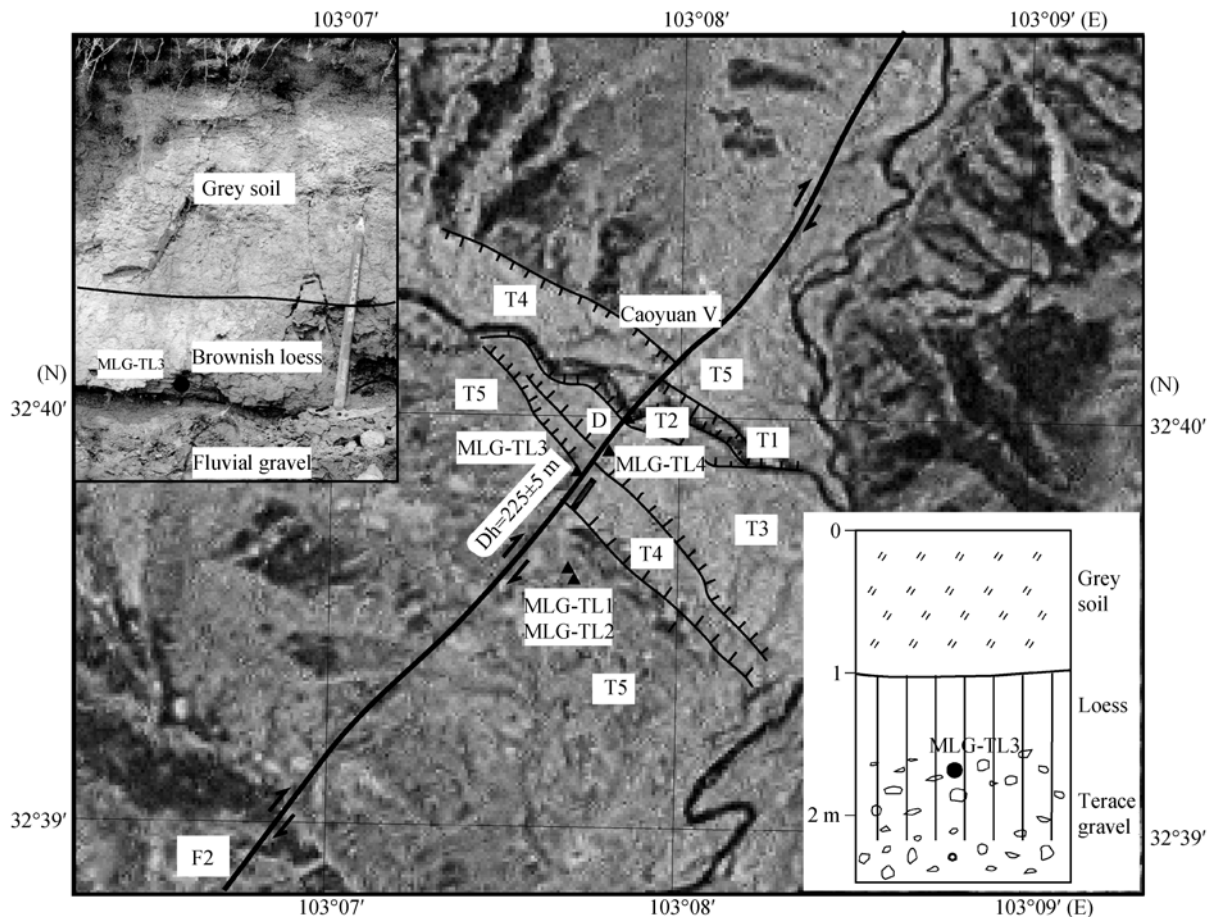


Figure 7 Interpreted ETM satellite images of the Maoergai fault and offset landforms west of Caoyuan Village to the northeast of Maoergai Town. The location is shown in Figure 2. Coarse black line represents the fault. Black triangle indicates the sampling locations and number of dating samples. Zigzag black lines represent terrace risers. T1, T2, T3 and T4 are the terraces from younger to older. Inset diagram at the upper left corner is the photo for sample MLG-TL3 and that at the lower right corner the sampling cross section for the T3 terrace. The location of the figure is indicated in Figure 2.

southern wall its height is only 1.5–2 m. Moreover, the age of the sample collected from the bottom of fine-grained superjacent cover on the fluvial gravel layer of the T4 terrace is 20.7 ± 2.2 ka, which is older than the formation time of the T3 terrace. Based on the age data for the adjacent terraces in the vicinity of Gema Village and regional paleoclimate variation^[38,39], it is postulated that the T3 terrace was formed at about 13.1 ± 1.7 ka BP. According to the 48 ± 5 m cumulative right-lateral offset (Figure 8) and the 13.1 ± 1.7 ka age of the T4/T3 riser, it can be estimated that the average right-lateral slip rate for the Maoergai fault in the late Pleistocene and Holocene is 3.6 ± 0.5 mm/a. In addition, if the age of about 74.5 ± 8.5 ka for the T5 terrace is taken as the upper limit of the beginning time of the 225 ± 15 m right-lateral displacement of the T5/T4 riser, then the average right-lateral slip rate for this fault since late Pleistocene can be estimated as greater than 3.0 ± 0.45 mm/a, which

can be used to test the aforementioned slip rate.

2.3 Kinetic features and formation time

Field investigations, measurements of offset landforms and sample dating have shown that the northern branch fault of the Longriba fault zone, the Longriqu fault, has relatively large reverse component, and the vertical slip rate along this fault is about 0.66 mm/a, corresponding to a NW-SE directing crustal shortening rate of about 0.55 mm/a. The right-lateral strike-slip rate along this fault is about 4.0 ± 0.1 mm/a. The southern branch fault, the Maoergai fault, is a pure strike-slip fault, along which the average right-lateral strike-slip rate is about 3.6 ± 0.5 mm/a. According to vector synthesizing principle^[16], it can be estimated that the right-lateral strike-slip rate along the northeast segment of the Longriba fault zone is 5.4 ± 2.0 mm/a, the vertical slip rate is 0.66 mm/a, and the corresponding crustal shortening rate is 0.55 mm/a. The slip direction can be determined to be

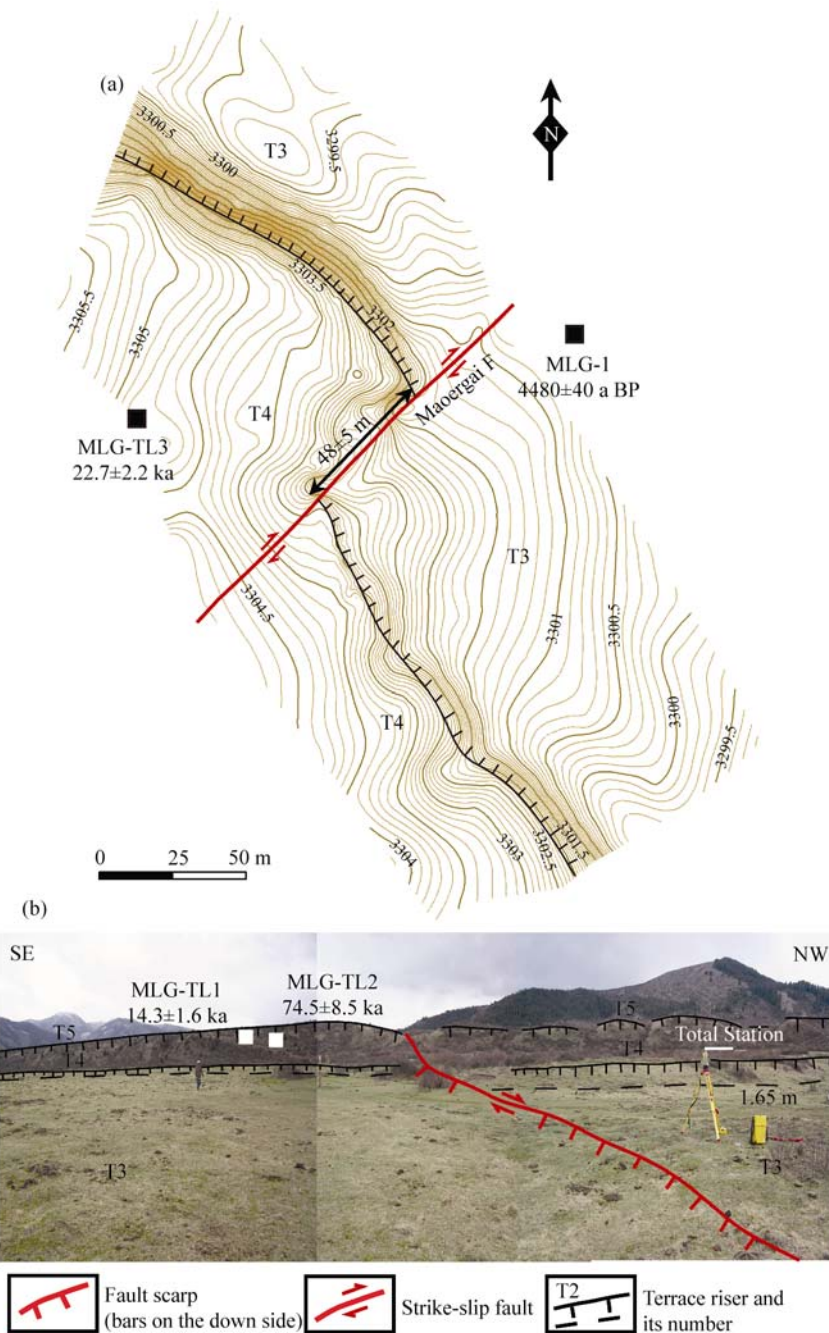


Figure 8 (a) Measured topographic map of right-laterally offset terraces along the Maoergai fault by using Total Station; (b) the corresponding photo (viewed to SWW). Location: the southwest of the Caoyuan Village about 9 km to the northeast of the Maoergai Village ($32^{\circ}39'55.1''\text{N}$, $103^{\circ}07'48.0''\text{E}$). The legends are the same as in Figure 5.

$\text{N}54^{\circ}\text{E}$. Thus, the geologic strike-slip rate obtained in this study is consistent well with GPS-monitored present-day shear strain rate^[31], but GPS monitoring does not reveal the existence of vertical motion on either side of the Longriba fault zone and nor does it reveal NW-SE directing crustal shortening.

On the ground, the northeast segment of the Longriba fault zone extends discontinuously. Along the NE-

trending Longriqu stream valley, which is partly controlled by the downthrown side of the Longriqu northern branch fault, there exist mainly Triassic strata, overlain by Late Pleistocene to Holocene fluvial deposits. The age of the samples collected from the raised fluvial fan apex is only 15 ka, while the depositing time of the highest terrace on the northwest bank of the Maoergai River, which was offset by the Maoergai fault, is dated

to be 75 ka. No older deposits were found in this area. All these data may indicate that the Longriba fault zone is a newly generated fault zone that has initiated since late Quaternary. Although it is relatively small in scale, its average right-lateral slip rate of 5.6 ± 2.0 mm/a may indicate that the fault zone is currently very active.

3 Discussion

The discovery of the existence of the Longriba fault zone is of great importance for understanding of the tectonic deformation pattern of the eastern Bayan Har block, and especially of the Longmenshan sub-block, as well as to the further discussion on the features of the active tectonics along the eastern margin of the Qinghai-Tibet Plateau.

As shown in Figure 1, under the regional dynamic background of the uplift and eastward or southeastward extrusion of the blocks within the central Qinghai-Tibet plateau owing to the northward motion of the Indian Plate and collision with the Eurasian Plate^[1,3,4], the eastward or east-southeastward extrusion of the Bayan Har block was intensely resisted by the South China block. During the early and middle stages of late Cenozoic, tectonic movement dominated by thrusting and nappe occurred along the middle-south segment of the Longmenshan thrust, which follows the Mesozoic orogenic belt between the two blocks, and the Minjiang fault, resulting in the remarkable offset of the Neogene and early Quaternary strata along the two fault zones^[40,41], as well as the formation of the Chengdu Plain, which is the Cenozoic foreland basin of the middle-south segment of the Longmenshan thrust (Figure 1). Thick Pliocene and Pleistocene strata were deposited in the Chengdu basin, and they are significantly deformed and offset^[40]. However, offset landforms that have been formed since late Pleistocene along the two fault zones are less distinct. Among them, both the right-lateral strike slip and vertical slip rates for the middle-south segment of the Longmenshan thrust are about 1.5 mm/a, while the left-lateral strike-slip and vertical (reverse) slip rates along the Minjiang fault are 1.6 ± 0.2 and 0.5 mm/a^[36,42], respectively. At the same time, the thickness of late Quaternary strata within the Chengdu basin is very limited or locked, and the deformation and offset features of the strata are indistinct^[42,43]. All these phenomena indicate that since late Pleistocene the interaction between the Bayan Har block and South China

block along the middle-south segment of the Longmenshan thrust and the Minjiang faults has weakened significantly. The weakening might be related to the progressive development of the Longriba fault zone since the late Quaternary.

The geologic evidence provided in this study reveals that the Longriba fault zone has partitioned the most part of eastward or east-southeastward horizontal extrusion of the Bayan Har block into the right-lateral faulting at a rate of 5.6 ± 2.0 mm/a, and NW-SE crustal shortening at a rate of 0.55 mm/a. The present day GPS re-measurements^[31] have also shown that the Bayan Har block is significantly partitioned by the Longriba fault zone (Figure 9(a)). It can also be inferred from Figure 9(a) that through the partitioning on the Longriba fault zone, the remaining small eastward motion is absorbed partly by the Longmenshan sub-block between the Longmenshan thrust and Longriba fault zone, and transformed into the faulting and vertical uplift within the sub-block. Finally, the very small remaining part of the motion has become the driving force of the modern movement along the middle-south segment of the Longmenshan thrust.

The seismic soundings show that the Longriba fault zone is the southern boundary of the lower-velocity anomaly areas in middle-upper crust in Ahba Region. The main fault plane of the Longriba fault zone dips toward the NW and its dip angle decreases with depth until it becomes a decollement on the top of a low-velocity body buried at 15–20 km depth^[44,45]. Finally, the fault zone has become the boundary between the Ahba and Longmenshan sub-blocks (Figure 9(b)). The Longmenshan sub-block itself is separated from the South China Block by the NW-dipping Longmenshan thrust. Its decollement is also on the top of the low-velocity body in middle-upper crust^[19]. Moreover, the rapid uplifting and cooling of the Longmen Mountain occurred during 11–5 Ma, while those of the Minshan Mountain and its surrounding areas occurred during 5–3 Ma, implying that the rapid cooling becomes younger westward from the Longmen Mountain, which is close to the Chengdu Plain^[34]. All these results make it possible to propose a slip partitioning model for interpreting the relationship between the middle-south segment of the Longmenshan thrust and the Longriba fault zone in tectonic deformation and evolution. Figure 9(b) is an idealized NE-trending structural cross-section

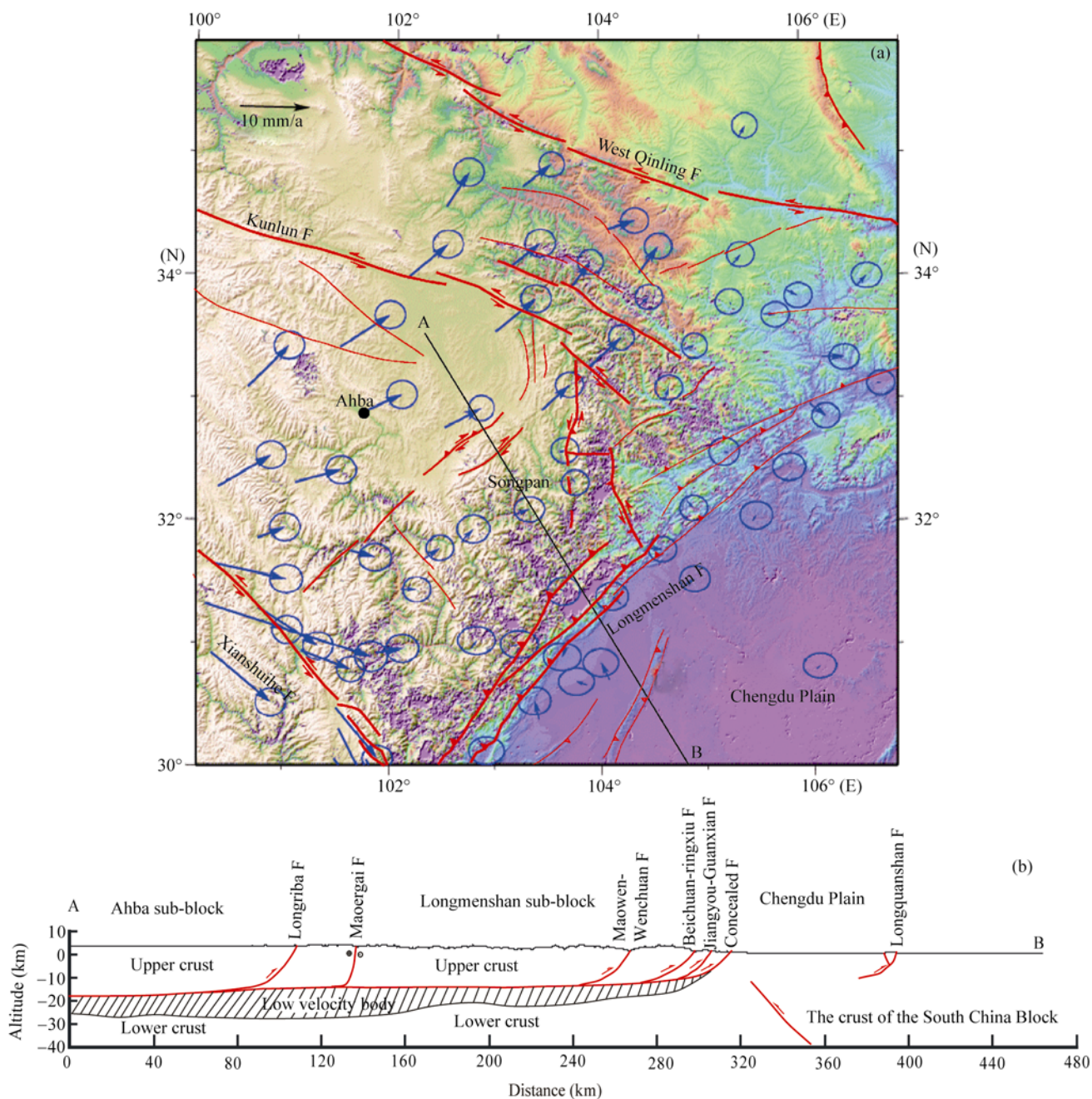


Figure 9 (a) GPS velocity field with respect to the South China Block in the eastern margin of the Qinghai-Tibet Plateau (1999–2001) and each velocity arrow originates at the location of the site and points to its motion direction. (b) Idealized structural cross-section of a backward propagated nappe tectonic system along the A-B traverse in Figure 9(a). Red lines represent active faults and blue arrows indicate GPS horizontal slip rate and its errors^[31].

along the A-B profile. It can be inferred from Figure 9(b) that owing to the intense resistance of the northwest corner of the South China block (the Chengdu basin), the late Cenozoic tectonic deformation on the eastern margin of the Qinghai-Tibet plateau has progressively propagated from the middle-south segment of the NE-trending Longmenshan thrust to the backland until the formation of Longriba fault zone in the backland about 200 km apart in the late Quaternary. During this

tectonic process, the middle-south segment of the Longmenshan thrust has become weaker in the late Quaternary. Therefore, the middle-south segment of the Longmenshan thrust, the Longriba fault zone and the Longmenshan sub-block bounded by them have made up the boundary tectonic zone of the eastern margin of the Qinghai-Tibet Plateau since late Quaternary. This boundary tectonic zone displays relatively strong tectonic and seismic activities.

Moreover, Figure 1 shows that only a few earthquakes have occurred on the Longriba fault zone and in the southwest of the Longmenshan sub-block, but this might be caused by lack of historical earthquake records for this highland. In fact, incomplete historical records of earthquake in the past 400 years are available only for the reaches of Minjiang River (Chengdu-Wenchuan-Songpan areas) and Fujiang River (Jiangyou-north Pingwu area) in the northeast of the Longmenshan sub-block. The aforementioned analysis and recognition of this study show that the Longriba fault zone and the Longmenshan sub-block possess the active tectonic and dynamic conditions for generating strong or large earthquakes.

4 Conclusions

The Longriba fault zone on the eastern margin of the Qinghai-Tibet Plateau is a strongly active right-lateral strike-slip fault newly-generated in the late Quaternary. The northeast segment of the fault zone consists of two parallel branch faults about 30 km apart. The northern branch fault, the Longriqiu fault, displays a relatively large reverse component, with an average right-lateral strike-slip rate of about 3.7 ± 0.3 mm/a and vertical slip

rate of 0.7 mm/a. The southern branch fault, the Maoergai fault, is a pure strike-slip fault, having an average right-lateral strike-slip rate of 3.6 ± 0.5 mm/a. The total average right-lateral slip rate along the northeast segment of the Longriba fault zone is estimated to be 5.4 ± 2.0 mm/a, the vertical slip rate to be about 0.7 mm/a, and the crustal shortening rate to be about 0.55 mm/a.

The Longriba fault zone was formed in the late Quaternary, when the backward propagated nappe tectonic system was developed northwestward from the middle-south segment of the NE trending Longmenshan thrust. The main cause is the intense resistance of the South China block to the southeastward extrusion of the Bayan Har block. During the formation of the Longriba fault zone, the middle-south segment of the Longmenshan thrust has progressively become weaker. Both the Longmenshan thrust and Longriba fault zone, together with the Longmenshan sub-block bounded in between, display a remarkable crustal shortening in a range of 200 km wide. This may imply that the backward propagated nappe tectonic system not only supports the current tectonic deformation on the eastern margin of the Qinghai-Tibet Plateau, but also controls the present-day activity of destructive earthquakes in the region.

- 1 Tapponnier P, Peltzer G, Le Dain A Y, et al. Propagating extrusion tectonics in Asia: New insights from simple experiments with plasticine. *Geology*, 1982, 10: 611–616
- 2 Peltzer P, Tapponnier P. Formation and evolution of strike-slip faults, rifts, and basins during the India-Asia collision—An experimental approach. *J Geophys Res*, 1988, 93(B10): 15085–15117
- 3 Avouac J P, Tapponnier P. Kinematic model of active deformation in central Asia. *Geophys Res Lett*, 1993, 20: 895–898
- 4 Tapponnier P, Xu Z, Roger F, et al. Oblique stepwise rise and growth of the Tibet Plateau. *Science*, 2001, 294(5547): 1671–1677
- 5 Replumaz A, Tapponnier P. Reconstruction of the deformed collision zone between India and Asia by backward motion of lithospheric blocks. *J Geophys Res*, 2003, 108 (B6): 2285, doi: 10.1029/2001JB000661
- 6 England P, McKenzie D. A thin viscous sheet model for continental deformation. *Geophys J Int*, 1982, 70 (2): 295–321
- 7 Houseman G, England P C. A Lithospheric Thickening Model for the Indo-Asian Collision. Cambridge: Cambridge University Press, 1996. 3–17
- 8 England P, Molnar P. The field of crustal velocity in Asia calculated from Quaternary rates of slip on faults. *Geophys J Int*, 1997, 130(3): 551–582
- 9 Royden L, Burchfiel B C, King R W, et al. Surface deformation and lower crustal flow in Eastern Tibet. *Science*, 1997, 276(5313): 788–790
- 10 Shen F, Leigh H R, Burchfiel B C. Large-scale crustal deformation of the Tibetan Plateau. *J Geophys Res*, 2001, 106 (B4): 6793–6816
- 11 Tapponnier P, Meyer B, Avouac J P, et al. Active thrusting and folding in the Qilian and decoupling between upper crust and mantle in the northeast Tibet. *Earth Planet Sci Lett*, 1990, 97: 382–403
- 12 Min W, Deng Q. The deformation characteristics of the Xiangshan-Tianjingshan fault and mechanism of compressional structures at the end of strike slip fault. In: Editorial Board of Research on Active Fault, ed. *Research on Active Fault* (in Chinese). Beijing: Seismological Press, 1991. 71–81
- 13 Meyer B, Tapponnier P, Bourjot L, et al. Crustal thickening in Gansu-Qinghai, lithospheric mantle subduction, and oblique, strike-slip controlled growth of the Tibetan Plateau. *Geophys J Int*, 1998, 135: 1–47
- 14 Wang E, Burchfiel C B, Royden L H, et al. Late Cenozoic Xianshuihe-Xiaojiang, Red River and Dali fault systems of southwestern Sichuan and central Yunnan, China. *Geological Society of America, Special Paper* 327, 1998. 108
- 15 Xu X W, Wen X, Zheng R, et al. Pattern of latest tectonic motion and its dynamics for active blocks in Sichuan-Yunnan region, China. *Sci China Ser D-Earth Sci*, 2003, 46 (Suppl. II): 210–226
- 16 Xu X W, Tapponnier P, Der Woerd J V. Late Quaternary sinistral slip rate along the Altyn Tagh fault and its structural transformation model. *Sci China Ser D- Earth Sci*, 2005, 48(3): 384–397
- 17 Yuan D, Zhang P, Liu B, et al. Geometrical Imagery and Tectonic

- Transformation of Late Quaternary Active Tectonics in Northeastern Margin of Qinghai-Xizang Plateau. *Acta Geol Sinica* (in Chinese), 2004, 78(2): 270–278
- 18 Chen S F, Wilson C J L, Deng Q D, et al. Active faulting and block movement associated with large earthquakes in Minshan and Longmenshan Mountains, northeastern Tibetan Plateau. *J Geophys Res*, 1994, 99(B12): 24025–24038
- 19 Song H. The comprehensive interpretations of geological and geophysical data in the orogenic belt of Longmen Mountains, China. *J Chengdu Inst Tech* (in Chinese), 1994, 21(2): 79–88
- 20 Zhao X, Deng Q, Chen S, et al. Tectonic geomorphology of the central segment of the Longmenshan thrust belt, Western Sichuan, Southwestern China. *Seismol Geol* (in Chinese), 1994, 16(4): 422–428
- 21 Deng Q, Chen S, Zhao X. Tectonics, seismicity and dynamics of Longmenshan Mountains and its adjacent regions. *Seismol Geol* (in Chinese), 1994, 16(4): 389–403
- 22 Jia D, Chen Z, Jia C, et al. Structural features of the Longmen shan fold and thrust belt and development of the western Sichuan foreland basin, central China. *Geol J China Univ* (in Chinese), 2003, 9(3): 402–409
- 23 Li Ch, Song F, Ran Y. Late Quaternary activity and age constraint of the northern Longmenshan thrust. *Seismol Geol* (in Chinese), 2004, 26(2): 248–258
- 24 Jia Q, Jia D, Zhu A, et al. Active tectonics in the Longmen thrust belt to the eastern Qinghai-Tibet Plateau and Sichuan basin: evidence from topography and seismicity. *Chin J Geol* (in Chinese), 2007, 42(1): 31–44
- 25 Arne D B, Wilson W C, Chen S, et al. Differential exhumation in response to episodic thrusting along the eastern margin of the Tibetan Plateau. *Tectonophysics*, 1997, 280: 239–256
- 26 Kirby E, Reiners P W, Korl M A, et al. Late Cenozoic evolution of the eastern margin of the Tibetan Plateau: Inference from $^{40}\text{Ar}/^{39}\text{Ar}$ and (U-Th)/He thermochronology. *Tectonics*, 2002, 21(1): 10.1029/2002TC001246
- 27 Zhang P, Wang Q, Ma Z. GPS velocity field and active crustal blocks of contemporary tectonic deformation in continental China. *Earth Sci Front* (in Chinese), 2002, 9(2): 430–441
- 28 Wang X, Zhu W, Fu Y, et al. Present-time crustal deformation in China and its surrounding regions by GPS. *Chin J Geophys* (in Chinese), 2002, 45(2): 198–209
- 29 Lü J, Shen Z, Wang M. Contemporary crustal deformation and active tectonic block model of the Sichuan-Yunnan region, China. *Seismol Geol* (in Chinese), 2003, 25(4): 543–554
- 30 Zhang P, Shen Z, Wang M. Continuous deformation of the Tibetan Plateau from global positioning system data. *Geology*, 2004, 32(9): 809–912
- 31 Shen Z K, Lü J N, Wang M, et al. Contemporary crustal deformation around the southeast borderland of the Tibetan Plateau. *J Geophys Res*, 2005, 110 (B11409), doi: 10.1029/2004JB003421
- 32 Wen X, Xu X, Zheng R, et al. Average slip-rate and recent large earthquake ruptures along the Garzê-Yushu fault. *Sci China Ser D-Earth Sci*, 2003, 46(Suppl.): 276–288
- 33 Van der Woerd J, Ryerson F, Tapponnier P, et al. Uniform slip-rate along the Kunlun Fault: Implication for seismic behavior and large-scale tectonics. *Geophys Res Lett*, 2000, 27: 2353–2356
- 34 Kirby E, Harkins N, Wang E, et al. Slip rate gradients along the eastern Kunlun fault. *Tectonics*, 2007, 26: TC2010, doi:10.1029/2006TC002033
- 35 Yang X, Jiang P, Song F, et al. The evidence of the south Longmenshan thrusts cutting late Quaternary stratum. *Seismol Geol* (in Chinese), 1999, 21(4): 341–345
- 36 Zhou R, Li Y, Alexander L D, et al. Active tectonics of the eastern margin of the Tibet Plateau. *J Miner Petrol* (in Chinese), 2006, 26(2): 40–51
- 37 Jiang Z, Ma Z, Zhang X, et al. Recent horizontal movement and deformation in the northeast margin of Qinghai-Tibet block. *Chin J Geophys* (in Chinese), 44(5): 636–644
- 38 Yao T, Thompson L G, Shi Y, et al. Climate variation since the Last Interglaciation recorded in the Guliya ice core. *Sci China Ser D-Earth Sci*, 1997, 40(6): 662–668
- 39 Yao T D. Abrupt climate change in the latest glacial epoch in Qinghai-Tibet plateau: Comparative study of Guliya ice core and Greenland GRIP ice core. *Sci China Ser D-Earth Sci* (in Chinese), 1999, 29(2): 175–184
- 40 Li Y, Zhou R, Densmore A L, et al. Continental Dynamics and Geologic Responses on the Eastern margin of the Qinghai-Tibet Plateau (in Chinese). Beijing: Geological Publishing House, 2006. 1–146
- 41 Yang J, Deng T, Wang Y, et al. The Quaternary stress states over the upstream area of Minjiang River in Sichuan and its relation to earthquakes. *Seismol Geol* (in Chinese), 1979, 1(3): 68–75
- 42 Ma B, Su G, Hou Z, et al. Late Quaternary slip rate in the central part of the Longmenshan thrust from terrace deformation along the Minjiang River. *Seismol Geol* (in Chinese), 2005, 27(2): 234–242
- 43 Xu X W, Yu G, Ma W, et al. Model of latest crustal tectonic motion of the central tectonic zone on the mainland of China. *Earth Sci Front* (in Chinese), 2003, 10(Suppl): 160–167
- 44 Huang J, Zhao D. High-resolution mantle tomography of China and surrounding regions. *J Geophys Res*, 2006, 111, B09305, doi:10.1029/2005JB004066
- 45 Yuan X, Egorov A S. The Arctic Ocean-Eurasian Continent-Pacific Ocean Geoscience Transect. Beijing: Sciences Press, 2000